

# Anaerobic carbon oxidation in sediment of two Brazilian mangrove forests: the influence of tree roots and crab burrows

Erik Kristensen<sup>1,\*</sup>, Thomas Valdemarsen<sup>1</sup>, Paula C. de Moraes<sup>2</sup>, Arthur Z. Güth<sup>2</sup>, Paulo Y. G. Sumida<sup>2</sup>, Cintia O. Quintana<sup>1</sup>

<sup>1</sup> Department of Biology, University of Southern Denmark, Campusvej 55, Odense M, 5230, Denmark

<sup>2</sup> Instituto Oceanográfico da Universidade de São Paulo, Praça do Oceanográfico, 191, Cidade Universitária, 05508-120, São Paulo, Brazil

\* Corresponding author: [ebk@biology.sdu.dk](mailto:ebk@biology.sdu.dk)

## ABSTRACT

This study evaluated the effects of biogenic structures (tree roots and crab burrows) on sediment carbon (C), sulfur (S), and iron (Fe) biogeochemistry during the wet season in the Olaria mangrove forests near the city of Cananéia, São Paulo state, Brazil and the Nobrega mangrove forest approximately 2 km from the city. Anaerobic C oxidation pathways were assessed from sediment profiles and anaerobic incubations and related to the abundance of biogenic structures in the form of pneumatophores and crab burrows. Porewater depth profiles of dissolved inorganic carbon (DIC) and  $\text{SO}_4^{2-}$  were less steep in the presence than absence of biogenic structures. While Fe(II) appeared unaffected by biogenic structures, Fe(III) levels were significantly higher in the upper 4 cm of the sediment in the presence than absence of vegetation and bioturbation. Surprisingly, the concentration of Fe(III) in this layer was 2-6 times higher in the Nobrega forest (6-13  $\mu\text{mol cm}^{-3}$ ) than in the Olaria forest (1.5-6.5  $\mu\text{mol cm}^{-3}$ ). Accordingly, depth integrated sulfate reduction (SR) tended to be highest at Olaria, while iron reduction (FeR) was highest at Nobrega. SR accounted for 54-83% of DIC production, with no difference between forested sites, while FeR accounted for 8-24% of DIC production, with a 2-3 times higher contribution in the Nobrega versus the Olaria forest. The results suggest that mangrove roots and crab burrows in mangrove sediments only promote FeR at the expense of SR in the Nobrega forest. It appears that anthropogenic discharge from Cananéia city may have overridden the impact of biogenic structures on sediment redox conditions at Olaria, thereby diminishing the role of FeR without strong stimulation of overall C oxidation rates.

**Descriptors:** Sulfate reduction, iron reduction, biogeochemistry, mangrove roots, crab burrows.

## INTRODUCTION

Mangrove ecosystems are characterized by dense populations of highly productive trees and shrubs growing worldwide in tropical and subtropical climates, covering a total of 130,000 to 150,000  $\text{km}^2$  (Giri et al., 2011; Spalding et al., 2011; Friess et al., 2019). Mangrove forests in Brazil cover an

estimated area of 10,000-13,000  $\text{km}^2$  and extend over 90% of the coastline (Spalding et al., 2011; Schaeffer-Novelli et al., 2016). The ecological functioning of mangrove environments has been described for a variety of regions in Brazil, primarily with focus on features such as forest production, tree species distribution, fauna composition, trophic structure, nutrient cycling, and sediment composition (e.g., Ferreira et al., 2010; Schwamborn and Giarrizzo, 2015; Bernardino et al., 2016; Ximenes et al., 2016; Quadros et al., 2019). However, research on the dynamics of sediment

Submitted: 21-April-2022

Approved: 19-Oct-2022

Associate Editor: Elisabete S. Braga



© 2023 The authors. This is an open access article distributed under the terms of the Creative Commons license.

biogeochemistry in mangrove sediments with respect to transformation of carbon (C), iron (Fe), and sulfur (S) is still scarce in Africa and Central/South America, with current knowledge being primarily generated from Australasia, Asia, and North America (Kristensen et al., 2017). More data from the understudied regions, such as Brazil, are needed to achieve a complete global overview of mangrove biogeochemical functioning.

The input of organic C from various sources and its mixing within mangrove environments creates spatially heterogeneous sediments with complex microbial pathways (Alongi, 2014). Organic matter decomposition in mangrove sediments is mediated by microbial processes utilizing a variety of electron acceptors under a wide range of redox conditions, often modulated by high abundances of biogenic structures, such as tree roots and crab burrows (Kristensen and Alongi, 2006; Ferreira et al., 2007; Kristensen et al., 2011). Typically, aerobic and anaerobic microbial processes are each for 30-70% of benthic metabolism in mangrove sediment (Alongi et al., 2000; 2001). Anaerobic C oxidation processes are almost solely driven by Fe(III) and sulfate ( $\text{SO}_4^{2-}$ ) reduction, of which the former is responsible for 50-70% of total organic matter degradation in Fe-rich sediments (Kristensen et al., 2008; 2011; Quintana et al., 2015; Pan et al., 2019). Denitrification, manganese reduction, and methanogenesis are usually deemed unimportant for C cycling in mangrove environments due to nitrate and manganese limitation combined with high levels of  $\text{SO}_4^{2-}$  in sediment porewaters (Alongi et al., 2005; Canfield et al., 2005).

Tree roots and crab burrows are known to promote oxidation of sediments, which may stimulate the formation of reactive Fe oxides and hamper sulfide (HS<sup>-</sup>) accumulation in the upper 10-20 cm of the sediment (Nielsen et al., 2003; Kristensen and Alongi, 2006; Ferreira et al., 2007). These redox-dependent modifications are driven by rapid downward translocation of oxygen ( $\text{O}_2$ ) via aerenchyma tissues in roots and along crab burrow shafts during low tide air exposure (Kristensen and Alongi, 2006; Araujo et al., 2016; Cheng et al., 2020). However, it is still not fully understood how, and to what extent, increased redox conditions induced by biogenic structures affect C

oxidation pathways within mangrove sediments. Despite high levels of  $\text{O}_2$  within roots and burrows, the penetration depth into the surrounding sediment typically is less than few mm (Andersen and Kristensen, 1988; Michaels and Zieman, 2013). The primary effect of the translocated  $\text{O}_2$  is therefore not increased aerobic respiration, but instead reoxidation of metabolites, such as Fe(II), and increased Fe(III) respiration (Kristensen et al., 2000). It has been shown in vegetated and bioturbated *Spartina* saltmarshes that Fe(III) reduction may comprise up to 100% of total anaerobic sediment C oxidation, while  $\text{SO}_4^{2-}$  reduction dominates in areas devoid of plants and animals (Kostka et al., 2002; Gribsholt et al., 2003).

The aim of this study was to evaluate anaerobic sediment C oxidation pathways in two mangrove forests of differing distance from the city of Cananéia, São Paulo state, Brazil, with an emphasis on the effects of biogenic structures (tree roots and crab burrows). The sediment C, S, and Fe biogeochemistry of the Olaria and Nobrega mangrove forests was assessed and related to the abundance of biogenic structures by comparing forested locations having numerous pneumatophores and crab burrows with adjacent intertidal creek flats lacking these biogenic structures. We hypothesize that roots and crab burrows in mangrove sediments modify C oxidation pathways by promoting Fe(III) reduction at the expense of  $\text{SO}_4^{2-}$  reduction.

## METHODS

### STUDY LOCATIONS

The Cananéia lagoon is a complex mangrove-surrounded estuarine system located near the southern border of São Paulo state, Brazil (Fig. 1). The estuary has 110 km<sup>2</sup> of water area (mean depth of 6.5 m) that connects with the South Atlantic Ocean through the Cananéia inlet in the south and the Icapará inlet in the north, and that receives freshwater from a 1340 km<sup>2</sup> inland drainage basin (Schaeffer-Novelli et al., 1990). The Cananéia lagoon is surrounded by 72 km<sup>2</sup> of mangrove forests, confined to the inland perimeter and two islands (Cananéia and Comprida) (Cunha-Lignon et al., 2009). Water exchange in the estuary

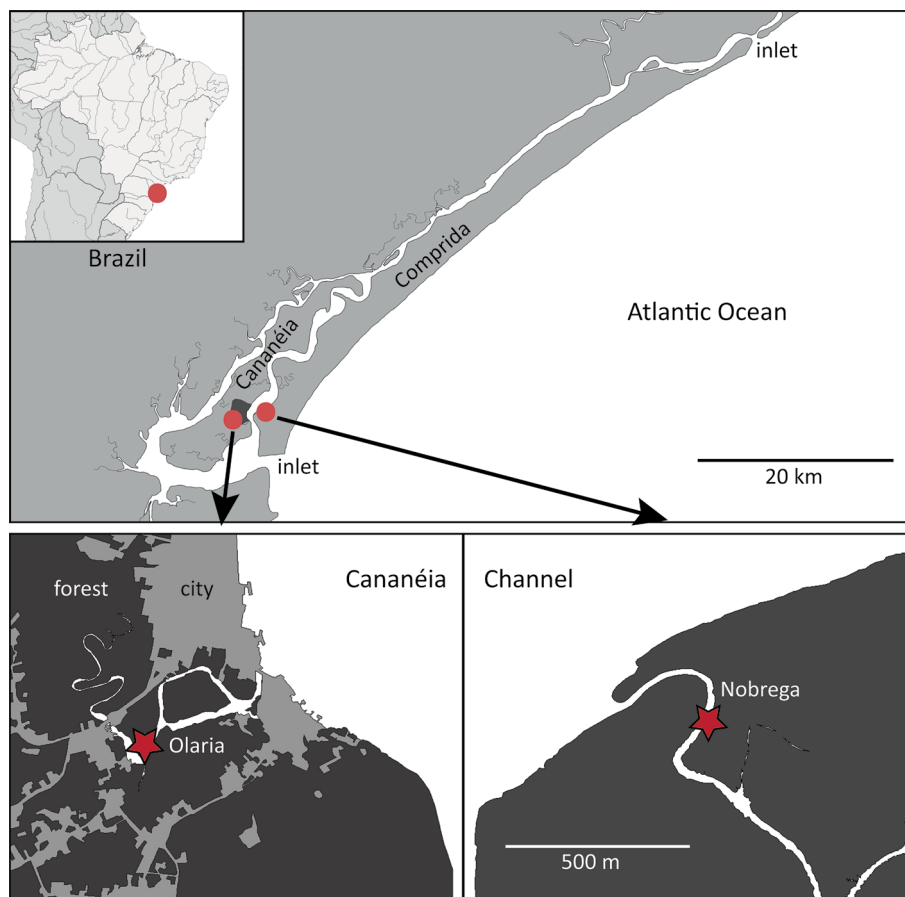


**Figure 1.** Map of Cananéia and Comprida Islands in Southern Brazil with blow-up of Olaria Creek in the vicinity of Cananéia City on Cananéia Island and Nobrega Creek on Comprida Island. The study locations are indicated by stars.

is driven by the tidal inflow of offshore seawater and the outflow of freshwater from several rivers and streams (Schaeffer-Novelli et al., 1990). Tides are semidiurnal, with an average amplitude of  $0.7 \pm 0.3$  m. The climate is mild subtropical, with an annual temperature range from 21 to 24°C, a typically wet summer (January to March), a dry winter (July to August), and average annual precipitation of 2200 mm (Cunha-Lignon et al., 2009).

The study was conducted in February 2014 along two mangrove creeks (Olaria and Nobrega) connected to the Cananéia channel. Olaria creek is near the small Cananéia City on Cananéia island, while Nobrega creek is located on the unpopulated Comprida island ca. 2 km from Cananéia island. The mangrove forests around both creeks are composed of three tree species, *Laguncularia racemosa*, *Rhizophora mangle*, and *Avicennia*

*schauerianna* (Schaeffer-Novelli et al., 1990). The most abundant burrowing mangrove crabs in the area belong to the families Ocypodidae (e.g., *Ucides cordatus* and *Uca* spp.) and Sesarmidae (e.g., *Aratus pisonii*).

Parallel samplings were conducted at two comparable mangrove locations in the Olaria (O) and the Nobrega (N) creeks (Fig. 1). The two locations were chosen for their similar vegetation and tidal elevation of the mangrove forest floor. Two intertidal sites were investigated at each creek location: the unvegetated narrow mud flat just outside the creek bank, and the mangrove forest floor 20 m inland of the creek, dominated by *Avicennia schauerianna*. Accordingly, the four examined sites were denoted Olaria mangrove floor (Site OF) and creek flat (Site OC) (25.0204 S, 47.9294 W), and Nobrega mangrove floor (Site NF) and creek flat (Site NC)

(25.0137 S, 47.9133 W). Site OF and NF were ~50 cm above mean sea level and were flooded 10-15 times every month during spring high tides. Site OC and NC were ~35 and ~25 cm above mean sea level, respectively, and were flooded during most high tides, except for 5-10 neap tides every month. Salinity and water temperatures were similar at the two locations (22.8-23.4 and 28-30°C, respectively) during the time of sampling.

### **PNEUMATOPHORES AND CRAB BURROW OPENINGS**

The density and size of visible biogenic structures (*Avicennia schauerianna* pneumatophores and burrow openings of unidentified crabs) were determined from digital photographs of the mangrove forest floor at OF (n = 14) and NF (n = 9). Each photograph included a known scale, covered on average 0.5 m<sup>2</sup> (range: 0.3 to 1 m<sup>2</sup>) of the forest floor, and was taken perpendicular to the sediment surface. All visible pneumatophores and burrow openings were counted through image analysis and used as a proxy for subsurface root and burrow presence.

### **SEDIMENT SAMPLING**

Sediment cores were collected from all sites by inserting 30 cm transparent core liners into the sediment. The cores were dug out by hand and closed on both ends with rubber stoppers before transport to the laboratory at the Universidade de São Paulo field station in Cananéia. Three sediment cores (20 cm deep, 5 cm inner diameter) were collected from each location for solid phase and porewater analyses, while another three sediment cores (20 cm deep, 8 cm inner diameter) were collected for anaerobic incubation (jar) experiments.

### **SEDIMENT CHARACTERISTICS AND POREWATER SOLUTES**

Three 5 cm inner diameter (i.d.) sediment cores from each site were sectioned into 1 cm intervals to 4 cm depth and 2 cm intervals to 18 cm depth (the 6-8 cm, 10-12 cm, and 14-16 cm sections were discarded for logistical reasons). Since the slicing was performed in air, the sediment

from each depth interval was immediately homogenized and subsampled for various analyses to avoid oxidation artefacts. Sediment wet density was determined as the weight of a known volume using cut-off syringes. Subsamples were analyzed for grain size using a Malvern Mastersizer 3000 Particle Size Analyzer with 0.5 % analytical precision. Water content was determined from the weight loss after drying (60°C) sediment samples until constant weight. Particulate organic carbon (POC) and total nitrogen (TN) content (analytical precision of 0.2 %) were determined for dried sediment samples on a Carlo-Erba CHN EA1108 Elemental Analyzer as described by Kristensen and Andersen (1987).

Reactive Fe was assessed from ~0.2 g subsamples by extraction in 0.5 M HCl for 30 minutes. The supernatant from Fe-extractions was analyzed for Fe(II) by the ferrozine method (Stookey, 1970), before (reactive Fe(II)) and after (total reactive Fe) reduction with hydroxylamine, as described by Lovley and Phillips (1987). The analytical precision was better than 5 µM. Reactive Fe(III) in the sediment was then determined as the difference between total reactive Fe and reactive Fe(II), assuming limited oxidation artefact by slowly diffusing O<sub>2</sub> during handling of the anoxic sediment.

The remaining sediment was transferred to centrifuge tubes and centrifuged (10 min, ~500 g). Porewater for DIC, SO<sub>4</sub><sup>2-</sup>, and Fe<sup>2+</sup> analyses was immediately after centrifugation siphoned from the centrifuge tubes with a syringe and GF/C-filtered. DIC samples were stored in gas tight containers until analysis by Gran titration within 24 hours of sampling (Talling, 1973) with an analytical precision better than 5 µM. Fe<sup>2+</sup> samples were acidified to pH < 1.5 with 0.5 M HCl and analyzed by the ferrozine method after reduction with hydroxylamine to avoid errors caused by oxidation in the extracted oxic porewater. SO<sub>4</sub><sup>2-</sup> samples were stored frozen (-20°C) and later analyzed by liquid ion chromatography on a Dionex ICS-2000 system with an analytical precision better than 10 µM. Stoichiometry of porewater DIC:SO<sub>4</sub><sup>2-</sup> was obtained from the least squares linear regressions of depth profiles.

## ANAEROBIC INCUBATIONS

The 8 cm i.d. sediment cores were sectioned into 2 cm intervals to a 18 cm depth. Only the sediment from the 0-2 cm, 4-6 cm, 8-10 cm, and 16-18 cm depth intervals was used in the assay. The sections from triplicate cores covering a surface area of 150 cm<sup>2</sup> were pooled (300 ml) and mixed thoroughly to obtain a sufficiently homogenized sediment representative for each depth interval. Eight 20 mL glass scintillation vials (“jars”) were fully packed with sediment from each interval, leaving no headspace. The jars were immediately closed with screw caps and taped to prevent O<sub>2</sub> intrusion before being incubated at 28°C in the dark. Sediment sectioning and handling was conducted as described above, but the bulk of the sediment remained anoxic throughout, except for the slow diffusion of O<sub>2</sub> into a thin outer layer.

Two jars from each depth were randomly chosen every 5-7 days for porewater and Fe-extraction. The screw cap was removed, and the upper 2 mm of sediment was discarded. Then, ~0.2 g of sediment was immediately transferred to 0.5 M HCl for Fe-extraction as described above. The jars were subsequently centrifuged head-up (10 min, ~500 g), and porewater was siphoned from the surface, filtered with GF/F filters and stored for later DIC and SO<sub>4</sub><sup>2-</sup> analysis as described above. The incubations provided a measure of anaerobic microbial reaction rates. The rates were quantified using

linear regressions of concentration changes as a function of incubation time. The regression slopes of DIC accumulation represent total anaerobic C oxidation, while slopes of Fe(III) and SO<sub>4</sub><sup>2-</sup> consumption represent Fe(III) reduction (FeR) and SO<sub>4</sub><sup>2-</sup> reduction (SR), respectively.

## STATISTICAL ANALYSIS

Significant differences between sampling sites (OF, OC, NF, and NC) were tested using one-way ANOVA for biogenic structures (pneumatophores and crab burrows) and solid phase parameters, while two-way ANOVA was used for depth profiles of porewater parameters and reactions rates. Data was tested for normality and homogeneity of variances before performing ANOVA tests. Tukey tests (pairwise post-hoc multiple comparisons) were applied between sampling sites when significant differences were detected by the ANOVAs. All tests were performed at a significance level of  $\alpha = 0.05$  using the software SigmaPlot 14.0.

## RESULTS

### SEDIMENT CHARACTERISTICS AND BIOGENIC STRUCTURES

The upper 18 cm of sediment consisted of fine-grained mud with similar characteristics at all sampling sites (Table 1). The median grain size ranged from 42-67  $\mu\text{m}$ , with a non-significant trend

**Table 1.** Sediment parameters and biogenic structures at Olaria and Nobrega mangrove forest and creek flat sites. Solid phase values are given as averages from depth profiles down to 18 cm into the sediment. Number of biogenic structures (pneumatophores and crab burrows) were counted from image analysis of sediment surface photos. Data are given as average ( $\pm$  sd). Variations in n are caused by differences in number of core replicates and depth intervals for solid phase parameters, and number of photos for biogenic structures.

Parameter	Olaria		Nobrega		n
	Forest (OF)	Creek Flat (OC)	Forest (NF)	Creek Flat (NC)	
Porosity	0.71 (0.04)	0.66 (0.04)	0.73 (0.04)	0.76 (0.06)	32
Median grain size ( $\mu\text{m}$ )	67 (12)	58 (21)	60 (20)	42 (9)	4
Silt+clay (%)	49.0 (3.9)	53.3 (10.6)	52.7 (7.3)	59.4 (5.4)	4
POC (% dw)	4.5 (0.5)	3.8 (0.8)	6.5 (0.6)	6.0 (0.8)	8
TN (% dw)	0.30 (0.05)	0.28 (0.09)	0.38 (0.03)	0.40 (0.07)	8
POC:TN (mol)	17.6 (1.6)	16.5 (2.2)	20.2 (1.6)	17.6 (1.1)	8
# Pneumatophores (m <sup>-2</sup> )	254 (204)	0	180 (23)	0	9-14
# Crab burrows (m <sup>-2</sup> )	125 (51)	0	89 (31)	0	9-14

for lower values at Nobrega than Olaria and with creek flat sites generally containing finer sediment than forest floor sites. Similarly, silt+clay content ranged between 49-59%, with a trend for higher levels in sediment from the Nobrega location and from the creek flat sites. Sediment POC and TN content were 3.8-6.5% and 0.28-0.40%, with significantly higher levels at the Nobrega location and no difference between the sites within each location. The molar POC:TN ratio was similar at 16.5-17.6 at all sites except NF, where a significantly higher level of 20.2 was reached.

The sediment surface at the forest sites (OF and NF) was perforated by numerous pneumatophores from the tree *Avicennia schauerianna* and burrows dug by ocypodid and sesamid crabs. The density of pneumatophores was approximately 200 m<sup>-2</sup> at both mangrove sites with slightly, albeit not significantly, higher numbers at OF than NF. Likewise, the 40 % higher density of crab burrow openings at OF (125 m<sup>-2</sup>) was not significantly higher than at NF (Table 1). Inspections of OC and NC creek flats revealed a complete absence of pneumatophores and crab burrow openings.

### POREWATER DIC AND SO<sub>4</sub><sup>2-</sup>

Porewater depth profiles of DIC and SO<sub>4</sub><sup>2-</sup> were highly different in sediments from the forest and

creek flat sites at both locations, but less so between the Olaria and Nobrega locations (Fig. 2). The steepest solute gradients were always observed at the creek flats, where the metabolite DIC accumulated with depth throughout the examined sediment depth, while the electron acceptor SO<sub>4</sub><sup>2-</sup> declined constantly in a similar fashion. Thus, DIC in the creek flat sediments increased from ≈2 mM at 0-1 cm to ≈25 mM (OC) and ≈20 mM (NC) at 16-18 cm depths (Fig. 2A). Porewater DIC in forest floor sediments accumulated similarly to the creek flat down to 5 cm, followed by a much slower increase with increasing depth, particularly at NF, to a level of ≈13 mM at 16-18 cm. Porewater SO<sub>4</sub><sup>2-</sup> near the sediment surface was significantly higher at the forest (22-23 mM) than at the creek site (14-18 mM) at both locations, and decreased with depth at all sites, showing almost a mirror image of DIC (Fig. 2B). The decline was similar and linear at both creek flat sites, reaching 4 mM at a 16-18 cm depth. SO<sub>4</sub><sup>2-</sup> depletion was less pronounced in the forest floor sediment, where OF only showed a decrease to 18 mM over the entire depth interval, while SO<sub>4</sub><sup>2-</sup> at NF decreased to 15 mM down to a 4-6 cm depth, with no further change with depth. Linear regressions between porewater profiles of DIC and SO<sub>4</sub><sup>2-</sup> were all significant (Fig. 3), with slopes ranging from -1.45 at NF to -2.31 at OF.

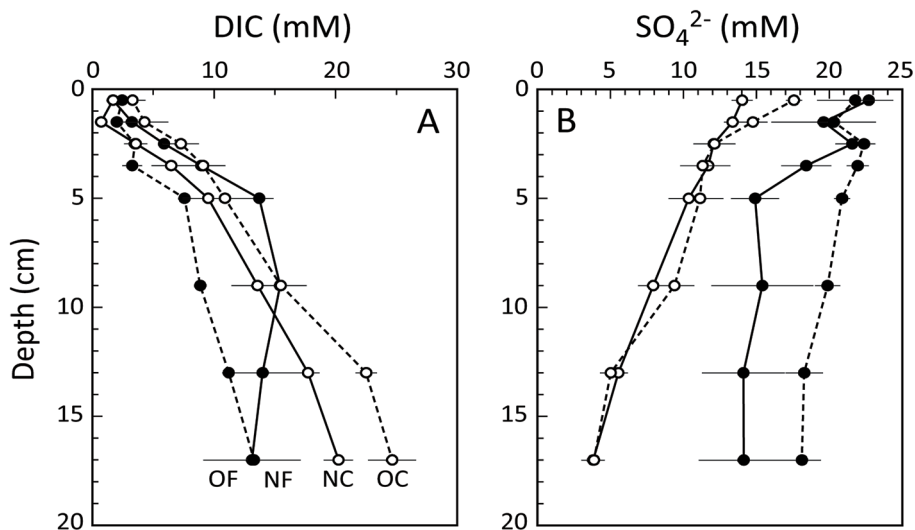


**Figure 2.** Vertical porewater solutes in sediment from Olaria forest (OF: filled symbols and broken lines), Olaria creek flat (OC: open symbols and broken lines), Nobrega forest (NF: filled symbols and full lines) and Nobrega creek flat (NC: open symbols and full lines). Panel A: DIC and panel B: SO<sub>4</sub><sup>2-</sup>. Error bars indicate ±SE.

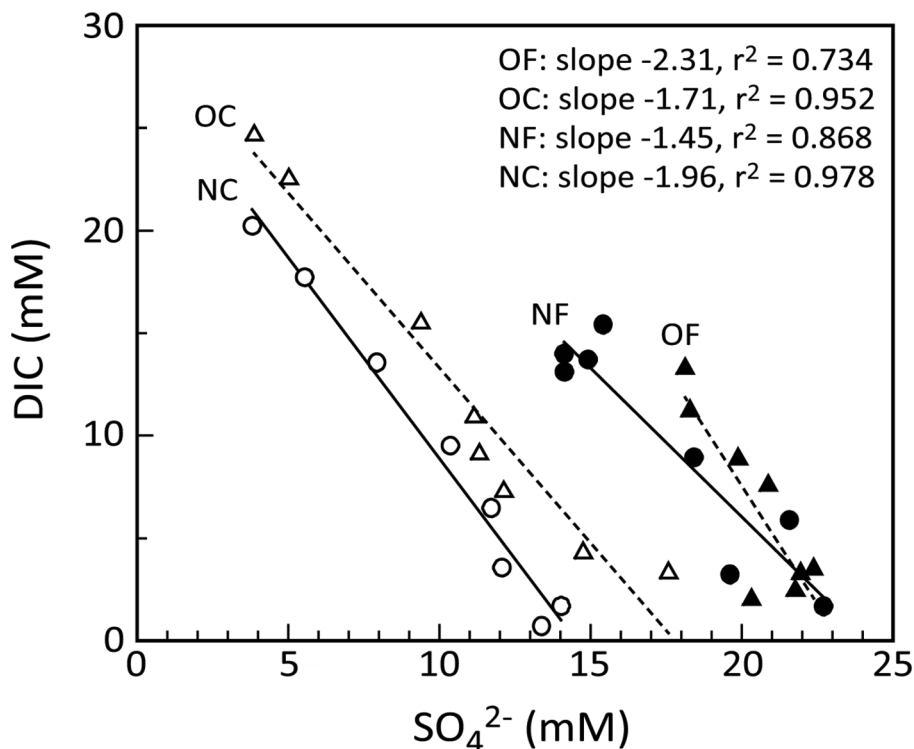


**Figure 3.** Plots between porewater solute profiles of DIC and  $\text{SO}_4^{2-}$  from the forested (solid symbols) and creek flat (open symbols) sites at the Olaria (broken lines) and Nobrega (full lines) locations. Slopes and correlation coefficients of the linear regressions are inserted.

### SOLID PHASE AND DISSOLVED IRON

Solid phase reactive iron (Fe(III) and Fe(II)) generally decreased with depth in the sediment (Fig. 4). Fe(II) was the dominant form, ranging from 10 to 45  $\mu\text{mol cm}^{-3}$  at both locations with significant differences between forest and creek flat sites only in the upper 1 cm, where Fe(II) at creek sites was 70-100 % higher than at forest sites (Fig. 4B,D). Sediment Fe(II) levels below 1 cm decreased with depth from 15-24  $\mu\text{mol cm}^{-3}$  to 9-16  $\mu\text{mol cm}^{-3}$  at all sites. Fe(III) was relatively low in the creek flat sediment at both OC and NC, with levels above 1.5  $\mu\text{mol cm}^{-3}$  only apparent in the upper 1 cm, reaching 8-11  $\mu\text{mol cm}^{-3}$  near the sediment-water interface (Fig. 4A, C). Fe(III) levels were significantly higher in the upper 4 cm of the vegetated and bioturbated forest floor at both locations. The concentration of Fe(III) in this layer was 2-6 times higher at NF (6-13  $\mu\text{mol cm}^{-3}$ ) than at OF (1.5-6.5  $\mu\text{mol cm}^{-3}$ ). Porewater  $\text{Fe}^{2+}$  levels were higher in the upper 5 cm at the Nobrega than at the Olaria sites (Fig. 5). A high concentration ( $\sim 140 \mu\text{M}$ ) was

evident near the surface at NC that declined to almost zero below 4 cm depth, while NF had a pronounced subsurface peak of  $>100 \mu\text{M}$  at 2-3 cm depth that declined and approached zero below 5 cm (Fig. 5B). Porewater  $\text{Fe}^{2+}$  was below 20  $\mu\text{M}$  at all depths at OF and only exceeded that level to 30-40  $\mu\text{M}$  in the upper 2 cm at OC (Fig. 5A).

### ANAEROBIC MICROBIAL C OXIDATION

The linear regressions of DIC,  $\text{SO}_4^{2-}$ , and Fe(III) concentration changes in jars as a function of incubation time were generally significant and with high correlation coefficients (Table 2). Only a few regressions (7 of 48) were not significant. Five of those were for Fe(III), pointing to a large bias for this solid phase parameter because of the relatively low Fe(III) concentrations in the small sediment subsamples. Solutes that were extracted from entire jars provide less uncertain results.

Total anaerobic C oxidation measured as DIC production in jars was highest near the sediment surface, reaching rates between 1.1-1.4  $\mu\text{mol cm}^{-3}$

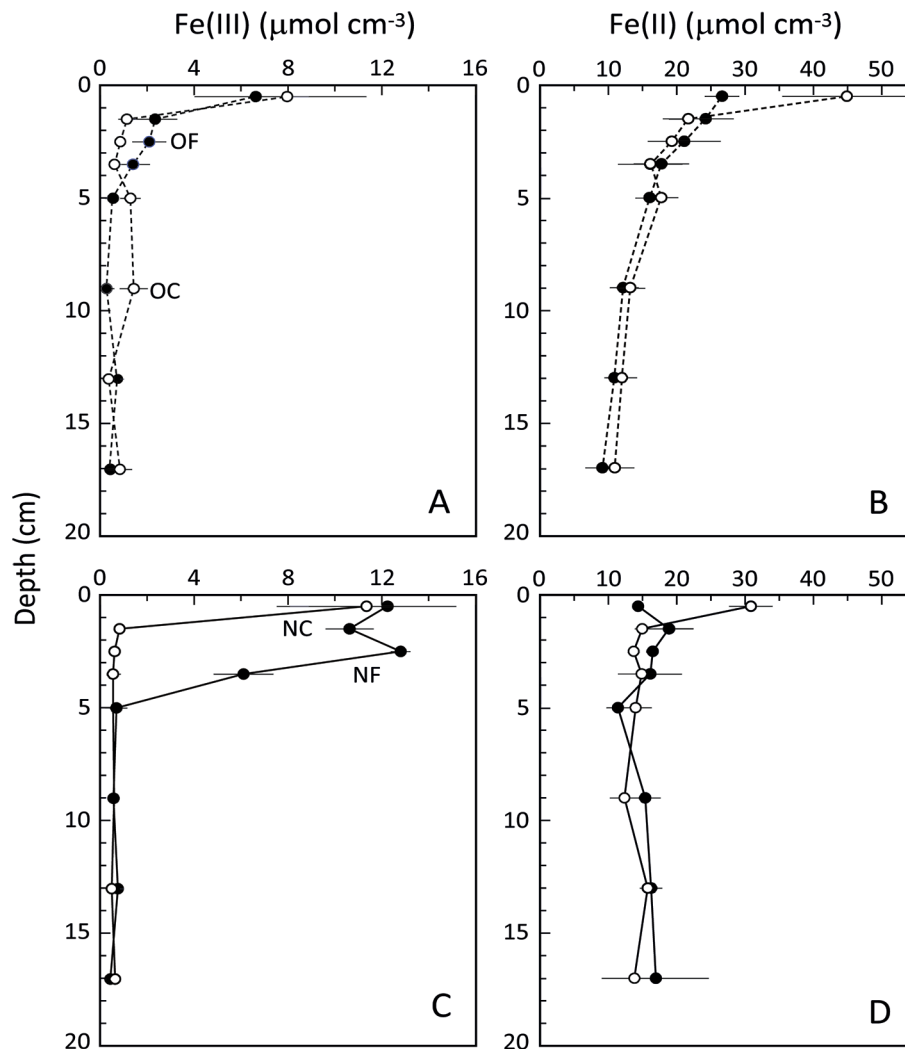


**Figure 4.** Vertical profiles of solid phase Fe(III) (A and C) and Fe(II) (B and D) in sediment from Olaria forest (OF: filled symbols and broken lines), Olaria creek flat (OC: open symbols and broken lines), Nobrega forest (NF: filled symbols and full lines) and Nobrega creek flat (NC: open symbols and full lines). Error bars indicate  $\pm$ SE.

$\text{d}^{-1}$  at 0-2 cm, except for NF that reached only  $0.7 \mu\text{mol cm}^{-3} \text{d}^{-1}$  (Fig. 6). Otherwise, rates of approximately  $0.5 \mu\text{mol cm}^{-3} \text{d}^{-1}$  below this depth were not significantly different among sites. These subsurface levels (below 2 cm depths) generally agreed with the sum of measured SR and FeR when converted to C units, i.e. using the theoretical stoichiometries of  $\text{SR} \times 2$  and  $\text{FeR} \times 1/4$  with fatty acids as substrates (Canfield et al., 2005). However, DIC production in the 0-2 cm depth interval was significantly higher than C oxidation by  $\text{SR} + \text{FeR}$ , except for NF. This near-surface difference was most pronounced at the creek sites, where  $\text{SR} + \text{FeR}$  only

reached 41% (OC) and 24% (NC) of DIC production, while the corresponding contributions at the forest sites were 58% (OF) and 80% (NF). The 0-18 cm depth-integrated rates of DIC production were not significantly different among the four Olaria and Nobrega mangrove sites (Table 3). Depth integrated SR tended to be highest at OF, but only significantly higher than at NC. Conversely, FeR was highest at NF, although not significantly different than at OC. SR accounted for 54-83% of DIC production at all sites, with higher contributions at forest (82-83%) than at creek (54-69%) sites. Accordingly, FeR was generally low at all sites,

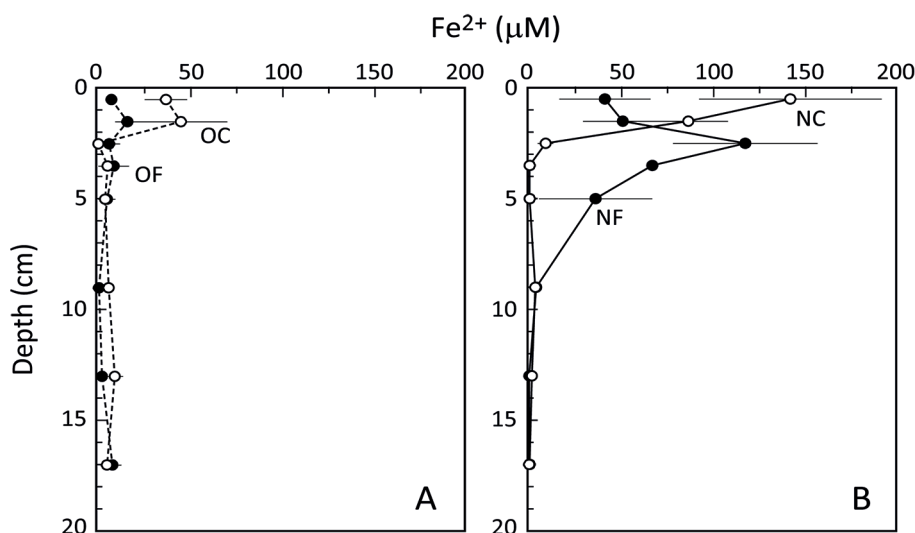


**Figure 5.** Vertical profiles of porewater iron ( $\text{Fe}^{2+}$ ). Panel A shows Olaria forest (OF) and creek flat (OC), and panel B shows Nobrega forest (NF) and creek flat (NC). Error bars indicate  $\pm$ SE.

**Table 2.** Correlation coefficients and significance levels of linear regressions between the examined jar compounds (DIC,  $\text{SO}_4^{2-}$  and  $\text{Fe(III)}$ ) and incubation time. Non-significant regressions are indicated by bold italics.

Compound	Depth (cm)	Olaria				Nobrega			
		Forest (OF)		Creek (OC)		Forest (NF)		Creek (NC)	
		$r^2$	p	$r^2$	p	$r^2$	p	$r^2$	p
DIC	0-2	0.79	0.017	0.97	<0.001	0.93	<0.001	0.95	<0.001
	4-6	0.78	0.002	0.88	<0.001	0.90	0.013	0.81	0.015
	8-10	0.94	<0.001	0.76	0.010	0.93	0.002	0.73	0.003
	16-18	0.89	0.005	0.64	0.017	0.70	0.020	0.78	0.021
$\text{SO}_4^{2-}$	0-2	0.88	0.005	0.99	<0.001	0.49	0.037	0.99	0.003
	4-6	0.97	<0.001	0.87	0.002	0.87	0.007	<b>0.29</b>	<b>0.134</b>
	8-10	0.70	0.001	0.79	0.001	0.83	0.004	0.83	0.002
	16-18	0.85	<0.001	<b>0.63</b>	<b>0.059</b>	0.71	0.017	0.81	0.006
Fe(III)	0-2	0.83	0.002	0.74	0.003	0.69	0.040	0.88	0.002
	4-6	0.90	<0.001	0.55	0.035	<b>0.35</b>	<b>0.091</b>	0.61	0.023
	8-10	0.64	0.003	0.52	0.028	<b>0.42</b>	<b>0.059</b>	0.53	0.041
	16-18	0.73	0.030	<b>0.39</b>	<b>0.072</b>	<b>0.24</b>	<b>0.154</b>	<b>0.23</b>	<b>0.188</b>

accounting for 8-24% of DIC production with a 2-3 times higher contribution at the Nobrega forest site (NF) than at all other sites.

## DISCUSSION

The rates of anaerobic C oxidation in sediments of the subtropical Olaria and Nobrega forests

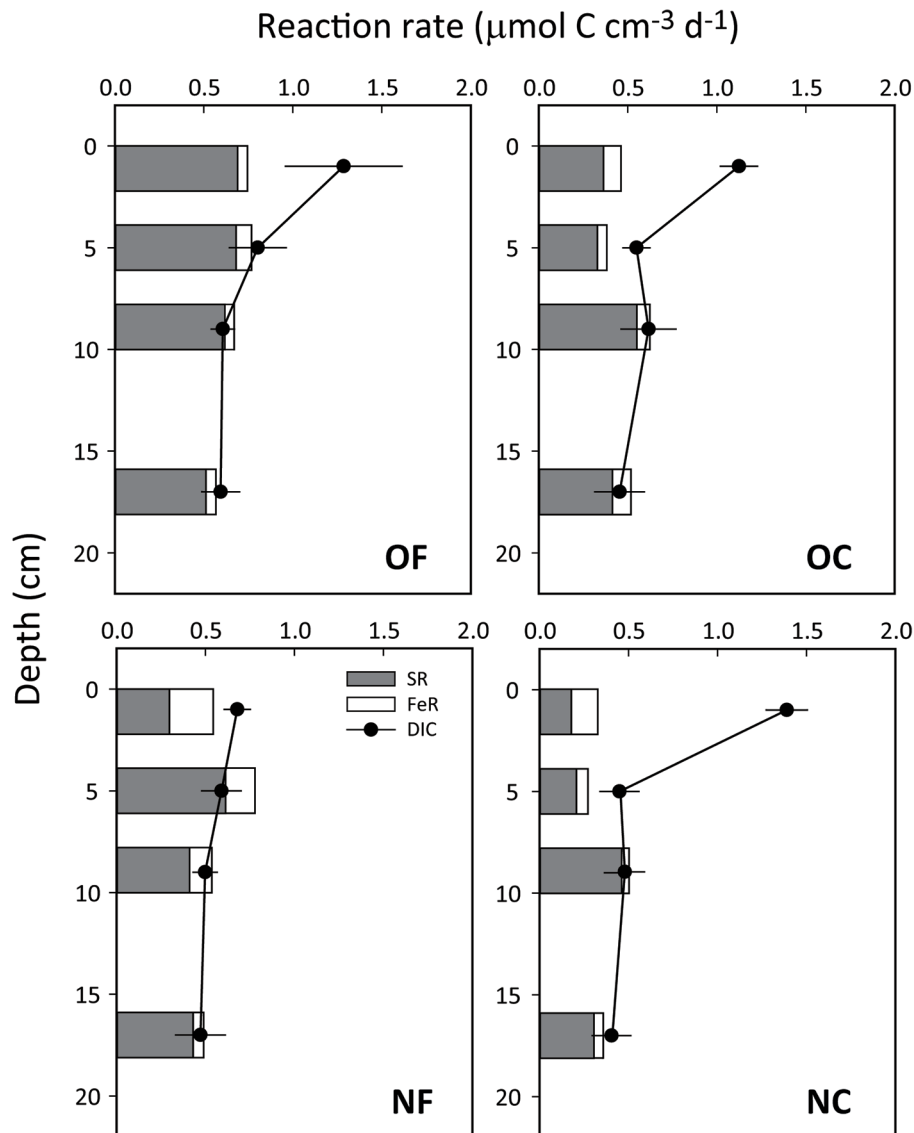


**Figure 6.** Depth profiles of C reaction rates from anaerobic incubations of sediment from Olaria forest (OF) and Olaria creek flat (OC) in upper panels, and Nobrega forest (NF) and Nobrega creek flat (NC) in lower panels. Symbols and full lines represent total DIC production (mean  $\pm$  SE). Grey bars represent SR and white bars represent FeR, both given as C equivalents.

during the warm wet season (Table 3) are within the range of those observed in tropical mangrove environments (Alongi et al., 2000; Kristensen et al., 2000; 2011; Alongi, 2020). Litterfall and associated benthic metabolism are considerably lower during the cold dry season, when the average temperature is 8°C lower than during the warm wet season, as argued by Rovai et al. (2021) and Kristensen et al. (2022). In any case, the depth-integrated anaerobic DIC production in the upper 18

cm of the Olaria and Nobrega creek flat (OC and NC) sediments during the warm season is not significantly affected by biogenic structures (Fig. 6). The rates were only 5–22 % lower than the daily average sediment/air  $\text{CO}_2$  and sediment/water DIC fluxes measured at the same locations during the warm season by Kristensen et al. (2022). This is surprising because SR certainly must be active below 18 cm and drive anaerobic C oxidation deep in these sediments. Thus, Alongi et al. (2005)

**Table 3.** Depth integrated reaction rates ( $\text{mmol C m}^{-2} \text{d}^{-1}$ ) of DIC production, SR and FeR in the upper 20 cm of sediment from the examined four Cananéia sites. Rates are averages based on slopes of porewater  $\text{TCO}_2$  accumulation and  $\text{SO}_4^{2-}$  depletion, as well as solid phase Fe(II) formation in anaerobic incubations over 3-4 weeks. Values in parentheses represent  $\pm$ SE of regression coefficients.  $\Delta$ DIC indicates the excess DIC production compared to C equivalents of  $\text{SRR} \times 2 + \text{FeR} \times 1/4$ . Finally, SR and FeR are given as the % of DIC production.

Parameter	Olaria		Nobrega		n
	Forest (OF)	Creek Flat (OC)	Forest (NF)	Creek Flat (NC)	
DIC	148.7 (27.5)	124.5 (22.7)	106.9 (20.5)	116.4 (22.0)	4
SR	121.6 (33.6)	86.2 (19.4)	88.2 (21.8)	62.4 (11.0)	4
FeR	12.2 (2.6)	16.6 (4.2)	25.8 (8.5)	13.5 (4.6)	4
$\Delta$ DIC	14.9	21.7	-7.1	40.5	-
SR in % of DIC	82	69	83	54	-
FeR in % of DIC	8	13	24	12	-

found relatively high rates of SR in mangrove sediments down to at least 1 m in depth. The depth integrated DIC production in both the Olaria and Nobrega forest sediments, on the other hand, only accounts for 34-51 % of the measured daily average flux (Kristensen et al., 2022). In these forested and bioturbated sediments, the remainder must be partly derived from deep (> 18 cm) microbial C oxidation as well as root and fauna respiration.

Another problem with the use of anaerobic jar incubations to determine C oxidation pathways is the exclusion of aerobic processes. The contribution of aerobic C oxidation in surface sediment exposed to  $\text{O}_2$  under *in situ* conditions is in jars replaced by anaerobic processes (e.g. FeR and SR). Since C oxidation is usually several fold faster under oxic than anoxic conditions (Hulthe et al., 1998; Kristensen and Holmer, 2001), the present jar rates must underestimate *in situ* rates. However, heterotrophic activity in mangrove sediments is usually sufficiently fast to prevent  $\text{O}_2$  penetration deeper than a couple of mm into the sediment (Brodersen et al., 2019). Accordingly, the underestimate caused by the absence of aerobic processes in jars from creek flats devoid of biogenic structures is limited because the bulk sediment remains anoxic anyway. The situation is reversed in the forest sediment, where the network of burrows and roots translocate  $\text{O}_2$  deep into the sediment and form a mosaic of oxic and anoxic niches (Kristensen and Alongi, 2006). The enhanced aerobic C oxidation from oxic subsurface sediment may here contribute to the abovementioned discrepancy between depth integrated DIC production from jars and *in*

*situ* fluxes. Nevertheless, Kristensen et al. (2000) observed that aerobic respiration contributed no more than 6 % of the total in mangrove sediment with high abundance of roots and burrows.

The higher DIC production in surface sediment (0-2 cm) than can be explained from SR and FeR is puzzling. The excess DIC in this reactive layer must be generated by other processes, such as fermentation (Valdemarsen and Kristensen, 2010) or respiration by manganese reduction and denitrification. Since the latter two respiration processes typically contribute less than 10 % of the total DIC production in mangrove sediments (Alongi et al., 2004; 2005), it is likely that most of the excess DIC production in the 0-2 cm jars is derived from fermentation in the reactive surface sediment.

The partitioning between FeR and SR in the Cananéia mangrove area differs from that observed elsewhere. The present study shows that FeR accounts for 8-24 % of the total anaerobic C oxidation in the upper 20 cm of the sediment, well below the level of up to 80 % observed by Kristensen et al. (2000; 2011) in Thailand and Tanzania. The key to understand and explain such large differences in the role of FeR is the content of reactive iron, and particularly available Fe(III), within the sediment. The studies of Kristensen et al. (2000; 2011) were from iron-rich mangrove environments with sediment Fe(III) concentrations of up to  $40 \mu\text{mol cm}^{-3}$ , well above the levels ( $< 10 \mu\text{mol cm}^{-3}$ ) found in the present study (Fig. 4). The differences in the contribution and rates of FeR among these environments therefore comply well with the global relationship between sediment FeR

in % of anaerobic C oxidation and the concentration of reactive Fe(III) as proposed by Jensen et al. (2003). It must be emphasized that this global relationship is based on volume-specific rates in the upper layers rich in Fe(III). Conversely, SR dominates in most mangrove environments when the area-based C oxidation is integrated to 1 m or deeper (Alongi et al., 2005).

Biogenic structures in the form of pneumatophores, with their supporting roots and deep crab burrows, are of pivotal importance for biogeochemical processes in mangrove sediments (Purnobasuki and Suzuki, 2004; Kristensen et al., 2008; Aschenbroich et al., 2017). They act as efficient conduits for gas exchange, particularly when sediments are air-exposed at low tide, leading to rapid diffusive subduction of  $O_2$  into subsurface sediment and enhanced oxidation Fe(II) and sulfides (Alongi et al., 2002; Kristensen and Alongi, 2006; Ferreira et al., 2007). Thus, the presently observed higher concentration of Fe(III) in the Nobrega forest floor (NF) than in the adjacent creek sediment (NC) clearly substantiates the role of biogenic  $O_2$  subduction for sediment redox conditions. While the capacity of roots for rapid delivery of  $O_2$  into subsurface sediment by diffusion through aerenchyma tissue is independent of inundation (Ferreira et al., 2007; Cheng et al., 2020), the non-ventilated crab burrows primarily channel  $O_2$  into the sediment during air exposure. Open burrows instead provide diffusive and advective solute exchange (i.e. DIC and  $SO_4^{2-}$ ) between the sediment and the overlying water during inundation (Aller, 1980; Furukawa et al., 2001; Kristensen et al., 2012).

Although biogenic structures have no apparent impact on the total microbial C oxidation at the Olaria and Nobrega locations, they have the potential to alter the balance between electron acceptor availability deep into the sediment (Robertson et al., 2009; Esch et al., 2013; Kristensen et al., 2018). Accordingly, the contribution of FeR to the total anaerobic C oxidation at Nobrega was twice as high in the forested (NF) than in the corresponding creek flat (NC) sediment (Table 3). A similar stimulation of FeR has been observed in other bioturbated and vegetated sediments (Kostka et al., 2002; Gribsholt et al., 2003). However, the

lack of elevated FeR at the forested site at Olaria (OF) is surprising when considering the similarity in density of potentially oxidizing pneumatophores and crab burrows. This discrepancy is probably caused by more reduced conditions in Olaria than in Nobrega sediments, as indicated by the low Fe(III) levels in the former (Fig. 4). Furthermore, the low porewater  $Fe^{2+}$  level in Olaria (Fig. 5) suggests that any available  $Fe^{2+}$  is rapidly removed by e.g. precipitated with sulfide instead of oxidation to Fe(III).

It is likely that the deposited organic matter at Olaria differs in quality from that at Nobrega. The mangrove forest surrounding Olaria creek is known to periodically receive sewage from suburban Cananéia city (Aidar et al., 1997; Barcellos et al., 2005). This deposition of anthropogenically derived organic matter may drive alternative biogeochemical processes that counteract the oxidizing capacity of biogenic structures at OF, and by doing so support higher SR and lower FeR. Furthermore, the substantially higher apparent DIC: $SO_4^{2-}$  stoichiometry in sediment porewater at OF (2.31) than at NF (1.45) suggests that the reactions involving organic C oxidation are different at the two locations (Fig. 3). The excess DIC generated at OF may not be delivered solely by SR but can, as mentioned above, also be generated by fermentation of fatty acids (Valdemarsen and Kristensen, 2010). The shutdown of sediment Fe(III) availability and FeR by anthropogenic discharges has been observed in other mangrove environments, even in the presence of oxidizing biogenic structures (Penha-Lopes et al., 2010; Kraal et al., 2015; Khirul et al., 2020).

The results from NF support our hypothesis that mangrove roots and crab burrows in mangrove sediments may promote Fe(III) reduction at the expense of  $SO_4^{2-}$  reduction. It is striking, however, that the potential anthropogenic influence at OF has apparently reduced mangrove sediment and overridden the oxidizing capacity of biogenic structures without any strong stimulation of the overall C oxidation rates. The exact underlying mechanisms for this biogeochemical phenomenon in the Cananéia mangrove forests are currently unknown and require further investigation.

## ACKNOWLEDGMENTS

We thank the technicians at the “Dr. João de Paiva Carvalho” field station, Instituto Oceanográfico of Universidade de São Paulo, for assistance during field sampling. The research was funded by the Danish Council for Independent Research (contract# 12-127012) to Erik Kristensen.

## AUTHOR CONTRIBUTIONS

E.K.: Conceptualization; Investigation; Funding acquisition; Writing – original draft; Writing – review & editing;

T.V. and C.O.Q.: Conceptualization; Investigation; Funding acquisition; Writing – review & editing;

P.C.M. and A.Z.G.: Investigation; Formal analysis; Project administration; Writing – review & editing;

P.Y.G.S.: Resources; Project administration; Writing – review & editing.

## REFERENCES

- AIDAR, E., SIGAUD-KUTNER, T. C. S., NISHIHARA, L., SCHINKE, K. P., BRAGA, M. C. C., FARAH, R. E. & KUTNER, M. B. B. 1997. Marine phytoplankton assays: effects of detergents. *Marine Environmental Research*, 43(1-2), 55-68.
- ALLER, R. C. 1980. Quantifying solute distributions in the bioturbated zone of marine sediments by defining an average microenvironment. *Geochimica et Cosmochimica Acta*, 44(12), 1955-1965.
- ALONGI, D. M. 2014. Carbon cycling and storage in mangrove forests. *Annual Review of Marine Science*, 6, 195-219.
- ALONGI, D. M. 2020. Carbon cycling in the World's mangrove ecosystems revisited: Significance of non-steady state diagenesis and subsurface linkages between the forest floor and the coastal ocean. *Forests*, 11(9), 977, DOI: <https://doi.org/10.3390/f11090977>
- ALONGI, D. M., PFITZNER, J., TROTT, L. A., TIRENDI, F., DIXON, P. & KLUMPP, D. W. 2005. Rapid sediment accumulation and microbial mineralization in forests of the mangrove *Kandelia candel* in the Jiulongjiang Estuary, China. *Estuarine, Coastal and Shelf Science*, 63(4), 605-618.
- ALONGI, D. M., SASEKUMAR, A., CHONG, V. C., PFITZNER, J., TROTT, L. A., TIRENDI, F., DIXON, P. & BRUNSKILL, G. J. 2004. Sediment accumulation and organic material flux in a managed mangrove ecosystem: estimates of land-ocean-atmosphere exchange in peninsular Malaysia. *Marine Geology*, 208(2-4), 383-402.
- ALONGI, D. M., TIRENDI, F. & CLOUGH, B. F. 2000. Below-ground decomposition of organic matter in forests of the mangroves *Rhizophora stylosa* and *Avicennia marina* along the arid coast of Western Australia. *Aquatic Botany*, 68(2), 97-122.
- ALONGI, D. M., TROTT, L. A., WATTAYAKORN, G. & CLOUGH, B. F. 2002. Below-ground nitrogen cycling in relation to net canopy production in mangrove forests of southern Thailand. *Marine Biology*, 140, 855-864.
- ALONGI, D. M., WATTAYAKORN, G., PFITZNER, J., TIRENDI, F., ZAGORSKIS, I., BRUNSKILL, G. J., DAVIDSON, A. & CLOUGH, B. F. 2001. Organic carbon accumulation and metabolic pathways in sediments of mangrove forests in southern Thailand. *Marine Geology*, 179(1-2), 85-103.
- ANDERSEN, F. Ø. & KRISTENSEN, E. 1988. Oxygen microgradients in the rhizosphere of the mangrove *Avicennia marina*. *Marine Ecology Progress Series*, 44, 201-204.
- ARAÚJO, J. M. C., FERREIRA, T. O., SUAREZ-ABELEDA, M., NÓBREGA, G. N., ALBUQUERQUE, A. G. B. M., BEZERRA, A. C. & OTERO, X. L. 2016. The role of bioturbation by *Ucides cordatus* crab in the fractionation and bioavailability of trace metals in tropical semiarid mangroves. *Marine Pollution Bulletin*, 111(1-2), 194-202.
- ASCHENBROICH, A., MICHAUD, E., GILBERT, F., FROMARD, F., ALT, A., LE GARREC, V., BIHANNIC, I., CONINCK, A. & THOUZEAU, G. 2017. Bioturbation functional roles associated with mangrove development in French Guiana, South America. *Hydrobiologia*, 794(1), 179-202.
- BARCELLOS, R. L., BERBEL, G. B. B., BRAGA, E. S. & FURTADO, V. V. 2005. Distribuição e características do fósforo sedimentary no sistema estuarino lagunar de Cananéia-Iguape, Estado de São Paulo, Brasil. *Geochimica Brasiliensis*, 19, 22-36.
- BERNARDINO, A. F., PAGLIOSA, P. R., CRISTOFOLLETTI, R. A., BARROS, F., NETTO, S. A., MUNIZ, P. & LANA, P. C. 2016. Benthic estuarine communities in Brazil: moving forward to long term studies to assess climate change impacts. *Brazilian Journal of Oceanography*, 64(spe 2), 81-96.
- BRODERSEN, K. E., TREVATHAN-TACKETT, S. M., NIELSEN, D. A., CONNOLLY, R. M., LOVELOCK, C. E., ATWOOD, T. B. & MACREADIE, P. I. 2019. Oxygen consumption and sulfate reduction in vegetated coastal habitats: effects of physical disturbance. *Frontiers in Marine Science*, 6, 14, DOI: <https://doi.org/10.3389/fmars.2019.00014>
- CANFIELD, D. E., KRISTENSEN, E. & THAMDRUP, B. 2005. *Aquatic geomicrobiology*. San Diego: Academic Press.
- CHENG, H., LIU, Y., JIANG, Z. Y. & WANG, Y. S. 2020. Radial oxygen loss is correlated with nitrogen nutrition in mangroves. *Tree Physiology*, 44(11), 1548-1560.
- CUNHA-LIGNON, M., MAHIQUES, M. M., SCHAEFFER-NOVELLI, Y., RODRIGUES, M., KLEIN, D. A., GOYA, S. C., MENGHINI, R. P., TOLENTINO, C. C., CINTRÓN-MOLERO, G. & DAHDOUH-GUEBAS, F. 2009. Analysis of mangrove forest succession, using sediment cores: a case study in the Cananéia-Iguape coastal system, Sao Paulo, Brazil. *Brazilian Journal of Oceanography*, 57(3), 161-174.

- ESCH, M. E. S., SHULL, D. H., DEVOL, A. H. & MORAN, S. B. 2013. Regional patterns of bioturbation and iron and manganese reduction in the sediments of the south-eastern Bering Sea. *Deep-Sea Research II*, 94, 80-94.
- FERREIRA, T. O., OTERO, X. L., SOUZA JUNIOR, V. S., VIDAL-TORRADO, P., MACÍAS, F. & FIRME, L. P. 2010. Spatial patterns of soil attributes and components in a mangrove system in Southeast Brazil (São Paulo). *Journal of Soils and Sediments*, 10(6), 995-1006.
- FERREIRA, T. O., OTERO, X. L., VIDAL-TORRADO, P. & MACÍAS, F. 2007. Effects of bioturbation by root and crab activity on iron and sulfur biogeochemistry in mangrove substrate. *Geoderma*, 142(1-2), 36-46.
- FRIESS, D. A., ROGERS, K., LOVELOCK, C. E., KRAUSS, K. W., HAMILTON, S. E., LEE, S. Y., LUCAS, R., PRIMAVERA, J., RAJKARAN, A. & SHI, S. 2019. The state of the World's mangrove forests: past, present, and future. *Annual Review of Environment and Resources*, 44, 89-115.
- FURUKAWA, Y., BENTLEY, S. J. & LAVOIE, D. L. 2001. Bioirrigation modeling in experimental benthic mesocosms. *Journal of Marine Research*, 59(3), 417-452.
- GIRI, C., OCHIENG, E., TIESZEN, L. L., ZHU, Z., SINGH, A., LOVELAND, T., MASEK, J. & DUKE, N. 2011. Status and distribution of mangrove forests of the world using earth observation satellite data. *Global Ecology and Biogeography*, 20(1), 154-159.
- GRIBSHOLT, B., KOSTKA, J. E. & KRISTENSEN, E. 2003. Impact of fiddler crabs and plant roots on sediment biogeochemistry in a Georgia salt marsh. *Marine Ecology Progress Series*, 259, 237-251.
- HULTHE, G., HULTH, S. & HALL, P. O. J. 1998. Effect of oxygen on degradation rate of refractory and labile organic matter in continental margin sediments. *Geochimica et Cosmochimica Acta*, 62, 1319-1328.
- JENSEN, M. M., THAMDRUP, B., RYSGAARD, S., HOLMER, M. & FOSSING, H. 2003. Rates and regulation of microbial iron reduction in sediments of the Baltic-North Sea transition. *Biogeochemistry*, 65, 295-317.
- KHIRUL, M. A., CHO, D. & KWON, S. H. 2020. Behaviors of nitrogen, iron and sulfur compounds in contaminated marine sediment. *Environmental Engineering Research*, 25(3), 274-280.
- KOSTKA, J. E., GRIBSHOLT, B., PETRIE, E., DALTON, D., SKELTON, H. & KRISTENSEN, E. 2002. The rates and pathways of carbon oxidation in bioturbated saltmarsh sediments. *Limnology and Oceanography*, 47(1), 230-240.
- KRAAL, P., BURTON, E. D., ROSE, A. L., KOCAR, B. D., LOCKHART, R. S., GRICE, K., BUSH, R. T., TAN, E. & WEBB, S. M. 2015. Sedimentary iron-phosphorus cycling under contrasting redox conditions in a eutrophic estuary. *Chemical Geology*, 392, 19-31.
- KRISTENSEN, E. & ALONGI, D. M. 2006. Control by fiddler crabs (*Uca vocans*) and plant roots (*Avicennia marina*) on carbon, iron and sulfur biogeochemistry in mangrove sediment. *Limnology and Oceanography*, 51(4), 1557-1571.
- KRISTENSEN, E. & ANDERSEN, F. Ø. 1987. Determination of organic carbon in marine sediments: a comparison of two CHN-analyzer methods. *Journal of Experimental Marine Biology and Ecology*, 109(1), 15-23.
- KRISTENSEN, E., ANDERSEN, F. Ø., HOLMBOE, N., HOLMER, M. & THONGTHAM, N. 2000. Carbon and nitrogen mineralization in sediment of the Bangrong mangrove area, Phuket, Thailand. *Aquatic Microbial Ecology*, 22(2), 199-213.
- KRISTENSEN, E., BOUILLON, S., DITTMAR, T. & MARCHAND, C. 2008. Organic carbon dynamics in mangrove ecosystems. *Aquatic Botany*, 89(2), 201-219.
- KRISTENSEN, E., CONNOLLY, R. M., OTERO, X. L., MARCHAND, C., FERREIRA, T. O. & RIVERA-MONROY, V. H. 2017. Biogeochemical cycles: Global approaches and perspectives. In: RIVERA-MONROY, V. H., LEE, S. Y., KRISTENSEN, E. & TWILLEY, R. R. (eds.). *Mangrove ecosystems: a global biogeographic perspective. Structure, function and ecosystem services*. Cham: Springer Nature, pp. 163-209.
- KRISTENSEN, E. & HOLMER, M. 2001. Decomposition of plant materials in marine sediment exposed to different electron acceptors ( $O_2$ ,  $NO_3^-$ , and  $SO_4^{2-}$ ), with emphasis on substrate origin, degradation kinetics, and the role of bioturbation. *Geochimica et Cosmochimica Acta*, 65(3), 419-433.
- KRISTENSEN, E., MANGION, P., TANG, M., FLINDT, M. R., HOLMER, M. & ULOMI, S. 2011. Microbial carbon oxidation rates and pathways in sediments of two Tanzanian mangrove forests. *Biogeochemistry*, 103(1-3), 143-158.
- KRISTENSEN, E., PENHA-LOPES, G., DELEFOSSE, M., VALDEMARSEN, T., QUINTANA, C. O. & BANTA, G. 2012. What is bioturbation? Need for a precise definition for fauna in aquatic sciences. *Marine Ecology Progress Series*, 446, 285-302.
- KRISTENSEN, E., RØY, H., DEBRABANT, K. & VALDEMARSEN, T. 2018. Carbon oxidation and bioirrigation in sediments along a Skagerrak-Kattegat-Belt Sea depth transect. *Marine Ecology Progress Series*, 604, 33-50.
- KRISTENSEN, E., VALDEMARSEN, T., MORAES, P. C., GÜTH, A. Z., SUMIDA, P. Y. G., QUINTANA, C. O. (2022) Pneumatophores and crab burrows increase  $CO_2$  and  $CH_4$  emission from sediments in two Brazilian fringe mangrove forests. *Marine Ecology Progress Series*, 698, 29-39. <https://doi.org/10.3354/meps14153>.
- LOVLEY, D. R. & PHILLIPS, E. J. P. 1987. Rapid assay for microbially reducible ferric iron in aquatic sediments. *Applied Environmental Microbiology*, 53(7), 1536-1540.
- MICHAELS, R. E. & ZIEMAN, J. C. 2013. Fiddler crab (*Uca* spp.) burrows have little effect on surrounding sediment oxygen concentrations. *Journal of Experimental Marine Biology and Ecology*, 448, 104-113.
- NIELSEN, O. I., KRISTENSEN, E. & HOLMER, M. 2003. Impact of *Arenicola marina* (Polychaeta) on sediment sulfur dynamics. *Aquatic Microbial Ecology*, 33, 95-105.

- PAN, F., LIU, H., GUO, Z., LI, Z., WANG, B., CAI, Y. & GAO, A. 2019. Effects of tide and season changes on the iron-sulfur-phosphorus biogeochemistry in sediment porewater of a mangrove coast. *Journal of Hydrology*, 568, 686-702.
- PENHA-LOPES, G., KRISTENSEN, E., FLINDT, M., MANGION, P., BOUILLON, S. & PAULA, J. 2010. The role of biogenic structures on the biogeochemical functioning of mangrove constructed wetlands sediments – a mesocosm approach. *Marine Pollution Bulletin*, 60(4), 560-572.
- PURNOBASUKI, H. & SUZUKI, M. 2005. Aerenchyma tissue development and gas-pathway structure in root of *Avicennia marina* (Forsk.) Vierh. *Journal of Plant Research*, 118(4), 285-294.
- QUADROS, A. F., NORDHAUS, I., REUTER, H. & ZIMMER, M. 2019. Modelling of mangrove annual leaf litterfall with emphasis on the role of vegetation structure. *Estuarine, Coastal and Shelf Science*, 218, 292-299.
- QUINTANA, C. O., SHIMABUKURO, M., PEREIRA C. O., ALVES, B. G., MORAES, P. C., VALDEMARSEN, T., KRISTENSEN, E. & SUMIDA, P. Y. G. 2015. Carbon mineralization pathways and bioturbation in coastal Brazilian sediments. *Scientific Reports*, 5, 16122.
- ROBERTSON, D., WELSH, D. T. & TEASDALE, P. R. 2009. Investigating biogenic heterogeneity in coastal sediments with two-dimensional measurements of iron(II) and sulfide. *Environmental Chemistry*, 6(1), 60-69.
- ROVAI, A. S., COELHO JUNIOR, C., ALMEIDA, R., CUNHA-LIGNON, M., MENGHINI, R. P., TWILLEY, R. R., CINTRÓN-MOLERO, G. & SCHAEFFER-NOVELLI, Y. 2021. Ecosystem-level carbon stocks and sequestration rates in mangroves in the Cananéia-Iguape lagoon estuarine system, southeastern Brazil. *Forest Ecology and Management*, 479, 118553, DOI: <https://doi.org/10.1016/j.foreco.2020.118553>
- SCHAEFFER-NOVELLI, Y., CINTRÓN-MOLERO, G., ADAIME, R. R. & CAMARGO, T. M. 1990. Variability of mangrove ecosystems along the Brazilian coast. *Estuaries*, 13, 204-218.
- SCHAEFFER-NOVELLI, Y., SORIANO-SIERRA, E. J., VALE, C. C., BERNINI, E., ROVAI, A. S., PINHEIRO, M. A. A., SCHMIDT, A. J., ALMEIDA, R., JÚNIOR, C. C., MENGHINI, R. P. R., MARTINEZ, D. I., ABUCHAHLA, G. M. O., CUNHA-LIGNON, M., CHARLIER-SARUBO, S., SHIRAZAWA-FREITAS, J. & CINTRÓN-MOLERO, G. 2016. Climate changes in mangrove forests and salt marshes. *Brazilian Journal of Oceanography*, 64(spe 2), 37-52.
- SCHWAMBORN, R. & GIARRIZZO, T. 2015. Stable isotope discrimination by consumers in a tropical mangrove food web: How important are variations in C/N ratio? *Estuaries and Coasts*, 38, 813-825.
- SPALDING, E. A., KAINUMA, M. & COLLINS, L. 2011. *World Atlas of Mangroves*. Kuala Lumpur: ITTO.
- STOOKEY, L. L. 1970. Ferrozine - a new spectrophotometric reagent for iron. *Analytical Chemistry*, 42(7), 779-781.
- TALLING, J. F. 1973. The application of some electrochemical methods to the measurement of photosynthesis and respiration in fresh water. *Freshwater Biology*, 3(4), 335-362.
- VALDEMARSEN, T. & KRISTENSEN, E. 2010. Degradation of dissolved organic monomers and short-chain fatty acids in sandy marine sediment by fermentation and sulfate reduction. *Geochimica et Cosmochimica Acta*, 74(5), 1593-1605.
- XIMENES, A., MAEDA, E. E., ARCOVERDE, G. F. B. & DAHDOUH-GUEBAS, F. 2016. Spatial assessment of the bioclimatic and environmental factors driving mangrove tree species' distribution along the Brazilian coastline. *Remote Sensing*, 8(6), 451, DOI: <https://doi.org/10.3390/rs8060451>